ELSEVIER

journal homepage: www.elsevier.com/locate/jmatprotec

Deformations of thin-walled plate due to static end milling force

*Tang Aijun**, *Liu Zhanqiang*

School of Mechanical Engineering, Shandong University, 73 Jingshi Road, Jinan 250061, China

ARTICLE INFO

Article history:
Received 11 June 2007
Received in revised form
6 November 2007
Accepted 15 December 2007

Keywords:
Deformations
Thin-walled plate
End milling

ABSTRACT

Many components used in the aerospace industry are usually thin-walled structures. Because of their poor stiffness, thin-walled parts are very easy to deform in the process of cutting. Due to the gradual reduced thickness during cutting, the end milling of thin-walled plate is a very complicated process. This paper proposes a new analytical deformation model suitable for static deformations prediction of thin-walled plate with low rigidity. The part deformations are predicted using a theoretical deformation equations model, which is established on the basis of reciprocal theorem when the linear load acts on thin-walled plates. The part deformations in end milling process are simulated by using FEM software ANSYS10.0. In the process of simulating, the influences of linear loads, location of the cutter (including x and y direction), thickness of the plates on the deformations of the thin-walled plates are analyzed. The results may help to increase the geometric accuracy of milling flexible thin-walled plates by considering the impact of the milling forces, location of cutter and the part thickness on the deformations of thin-walled structures. Furthermore, the results show that the diverse cutting parameters should be selected at each machining layer to satisfy the machining efficiency and precision in the process of milling thin-walled plate.
© 2007 Elsevier B.V. All rights reserved.

1. Introduction

With the higher demands on the speed and performance of the modern aircraft, the thin-walled aluminum alloy parts have been used broadly in aeronautics. Due to the large area and low rigidity, the thin-walled plates are always machined in numerical control (NC) end milling process. However, owing to various reasons in the machining process, the thin-walled plates are very easy to deform under the cutting force, which will influence the accuracy and quality. In end milling process, the thickness of the plates is reduced gradually, which makes it even more difficult to control the accuracy of machining. The end milling of such plates is complicated, where periodically varying milling forces excite the flexible plate structures both statically and dynamically and leading to significant deformations (Ratchev et al., 2005).

Several researches on the deformations of flexible parts have been done (Ratchev et al., 2005, 2006; Ning et al., 2003; Erhan and Altintas, 1995; Budak, 2006) in milling operations. Ratchev reports on an advanced error prediction and compensation strategy specifically focused on force-induced errors in machining of thin-walled structures (Ratchev et al., 2005, 2006). Ning applies the finite element method (FEM) to the quantitative analysis and calculation of the deformations of a typical thin-walled structure (a thin-walled box) in the process of machining, and proposes an NC compensation method to compensate for the deformations (Ning et al., 2003). Erhan–Budak models the peripheral milling of very

* *Corresponding author.*
E-mail address: tajsmile@sdjzu.edu.cn (T. Aijun).
0924-0136/$ – see front matter © 2007 Elsevier B.V. All rights reserved.
doi:10.1016/j.jmatprotec.2007.12.089

flexible, cantilevered plates with slender end mills, and considers partial separation of tool and plate structures due to static displacements (Erhan and Altintas, 1995; Budak, 2006).

However, the majority of previous research works in deformations of flexible parts have focused on the experimental and FE analysis. The goal of this paper is to propose a theoretical model to calculate the deformations in end milling of thin-walled plates on the basis of small deformations equations. The deformations are numerical simulated by using FEM software ANSYS10.0.

2. Static small deformations models of thin-walled plates in end milling

Very flexible plates are considered to have a large span ratio of height to thickness. The part to be machined in this paper discussed is only limited the small deformations of thin-walled plates. The thin-walled plates are that the thickness h is smaller than the minimal dimension of middle plane b, i.e. $(1/80\sim1/100)b \ll h \ll (1/8\sim1/5)b$. The small deformations are that the maximal deformation w is smaller than the thickness h, i.e. $w_{\max} \ll 0.2h$, which is to ensure the higher accuracy of the milled component and the range of elastic deformations.

In end milling of the thin-walled plates, the radial forces can be looked as the linear loads (see Fig. 1). The thin-walled plates in Fig. 1 can be considered as the cantilever plate, which is also the boundary condition for the plate.

For simplification, it applies the following assumptions for the calculation of small deformations of thin-walled plates:

(1) The displacement of every point on the plates does not change along the thickness, which is equal to the deformations of the plate middle plane.
(2) Straight normal line hypothesis: the normal line is still straight and vertical to the middle plane both pro-deformations and after deformations.

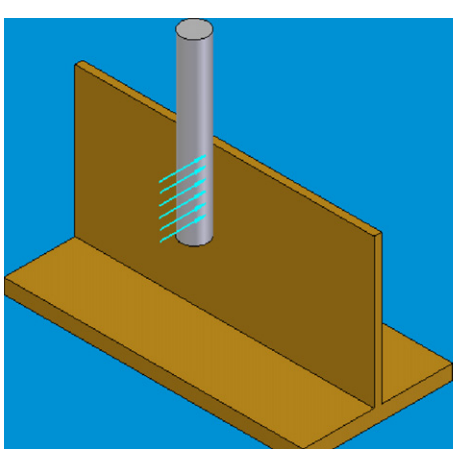

Fig. 1 – Linear loads acting on thin-walled plates.

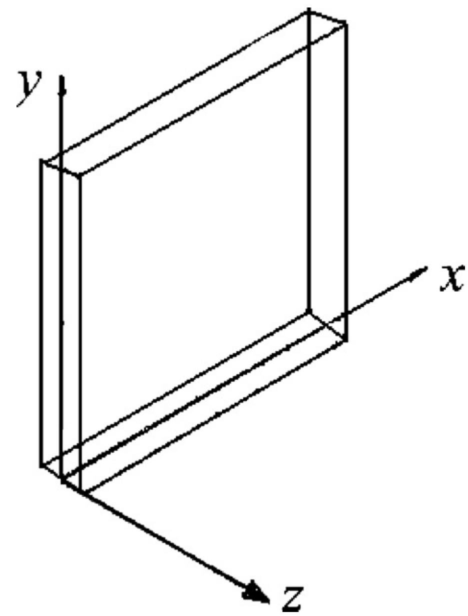

Fig. 2 – Coordinate system of cantilever plate.

(3) The normal stress applied on the plane that is parallel to the middle plane is very small. It thus can be ignored.

The oxy plane of the coordinate system coinciding with the middle plane of the plate is established. The direction of z-axis follows the right-hand rule (see Fig. 2).

In end milling of thin-walled plates, the periodical milling force excites the part dynamically. The influence of the cutting force components at x and y direction on the deformations is very tiny, which can be ignored. Therefore, this paper only considers the influence of radial cutting force on the z direction deformations. Accordingly, the unit linear load can be expressed by Eq. (1).

$$q = \frac{F_z}{a_p} = \frac{Nc}{8\pi}\left|K_{tc}(2\phi - \sin 2\phi) + K_{rc}\cos 2\phi\right|_{\phi_{st}}^{\phi_{ex}} \quad (1)$$

where N is the tooth number of cutter, c is the feed per tooth (mm/tooth), a_p is the axial depth of cutting(mm), ϕ is the immersion angle that varies with time, ϕ_{st} and ϕ_{ex} are the start and exit immersion angles of the cutter to and from the cutting zone, respectively. K_{tc} and K_{rc} are the milling force coefficients, F_z is the milling force in radial direction (N).

In order to use the reciprocal theorem between the cantilever plate system and basic system, the constraint of the fixed edge of cantilever plate is removed and replaced by the flexural torque M_0 (Fig. 3). As shown in Fig. 3, a denotes the length of thin-walled plates (mm), b denotes the width of thin-walled plates (mm), (x_0 and y_0) denotes the lowest contact point between the cutter and the plate, and q denotes the unit linear loads (N/m).

It can be assumed that the flexural torque value of fixed edge and the deformations of each free edge are formulated

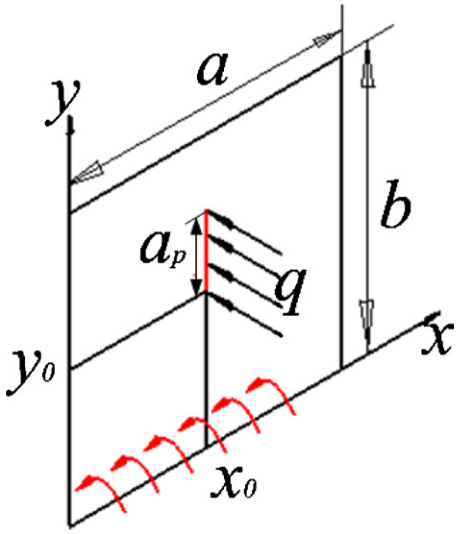

Fig. 3 – Actual system of cantilever plate.

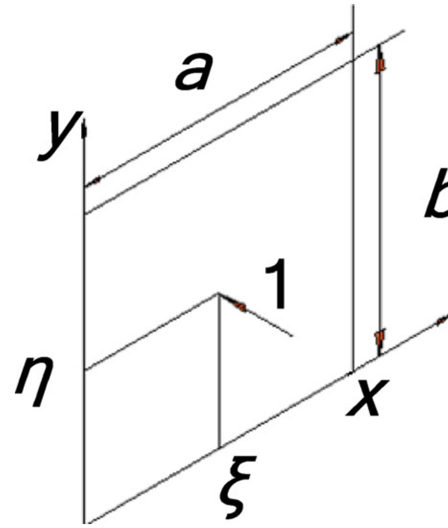

Fig. 4 – Basic system of rectangular plate.

by Eq. (2).

$$\begin{aligned} M_{y0} &= \sum_{m=1,2}^{\infty} C_m \sin \alpha_m x \\ w_{x0} &= \sum_{n=1,2}^{\infty} a_n \sin \beta_n y + \frac{y}{b} k_4 \\ w_{xa} &= \sum_{n=1,2}^{\infty} b_n \sin \beta_n y + \frac{y}{b} k_3 \\ w_{yb} &= \sum_{m=1,2}^{\infty} d_m \sin \alpha_m x + \frac{x}{a} k_3 + \frac{a-x}{a} k_4 \end{aligned} \quad (2)$$

where

$$\alpha_m = \frac{m\pi}{a}$$
$$\beta_n = \frac{n\pi}{b}$$

where C_m, a_n, b_n, d_m, k_3 and k_4 are unknown quantities, m and n are the positive integers.

The basic system of the rectangular plate can be shown in Fig. 4, a unit concentrated force acts on the mobile point (ζ and η) of the plane. On the basis of theory of reciprocal theorem between the actual system and basic system (Fu, 2003), the deformations Eq. (3) of actual system can be derived by the corresponding merger and transposition.

$$\begin{aligned} w(\xi, \eta) = &\int_{y_0}^{y_0+a_p} q w_1'(x_0, y; \xi, \eta) dy + \int_0^a M_{y0} w_{1,y0}' dx \\ &- \int_0^a V_{1yb}' w_{yb} dx - \int_0^b V_{1xa}' w_{xa} dy + \int_0^b V_{1x0}' w_{x0} dy \\ &+ R_{1ab}' k_3 - R_{10b}' k_4 = w_1 + w_2 + w_3 + w_4 + w_5 + w_6 \end{aligned} \quad (3)$$

where

$$w_1'(x_0, y; \xi, \eta) = \frac{4}{Dab} \sum_{m=1}^{\infty} \sum_{n=1}^{\infty} \frac{1}{K_{mn}'^2} \sin \alpha_m \xi \sin \beta_n \eta \sin \alpha_m x_0 \sin \beta_n y \quad (4)$$

$$w_{1,y0}' = \frac{4}{Dab} \sum_{m=1}^{\infty} \sum_{n=1}^{\infty} \frac{\beta_n}{K_{mn}'^2} \sin \alpha_m \xi \sin \beta_n \eta \sin \alpha_m x \quad (5)$$

$$V_{1yb}' = \frac{4}{ab} \sum_{m=1}^{\infty} \sum_{n=1}^{\infty} \frac{(-1)^n \beta_n}{K_{mn}'^2} [\beta_n^2 + (2-\mu)\alpha_m^2] \sin \alpha_m \xi \sin \beta_n \eta \sin \alpha_m x \quad (6)$$

$$V_{1xa}' = \frac{4}{ab} \sum_{m=1}^{\infty} \sum_{n=1}^{\infty} \frac{(-1)^m \alpha_m}{K_{mn}'^2} [\alpha_m^2 + (2-\mu)\beta_n^2] \sin \alpha_m \xi \sin \beta_n \eta \sin \beta_n y \quad (7)$$

$$V_{1x0}' = \frac{4}{ab} \sum_{m=1}^{\infty} \sum_{n=1}^{\infty} \frac{\alpha_m}{K_{mn}'^2} [\alpha_m^2 + (2-\mu)\beta_n^2] \sin \alpha_m \xi \sin \beta_n \eta \sin \beta_n y \quad (8)$$

$$R_{1ab}' = -\frac{8(1-\mu)}{ab} \sum_{m=1}^{\infty} \sum_{n=1}^{\infty} \frac{(-1)^{m+n} \alpha_m \beta_n}{K_{mn}'^2} \sin \alpha_m \xi \sin \beta_n \eta \quad (9)$$

$$R_{10b}' = -\frac{8(1-\mu)}{ab} \sum_{m=1}^{\infty} \sum_{n=1}^{\infty} \frac{(-1)^n \alpha_m \beta_n}{K_{mn}'^2} \sin \alpha_m \xi \sin \beta_n \eta \quad (10)$$

where

$$K_{mn}'^2 = (\alpha_m^2 + \beta_n^2)^2 - \lambda^2$$

$$D = \frac{Eh^3}{12(1-\mu^2)}$$

$$\lambda^2 = \frac{\rho\omega^2}{D}$$

By substituting Eq. (2), (4)–(10) into Eq. (3), the deformations equations are expressed as the bi-trigonometric series, respectively.

$$w_1 = -\frac{4q}{D\pi a}\sum_{m=1,2}^{\infty}\sum_{n=1,2}^{\infty}\frac{1}{nK'^2_{mn}}\sin\alpha_m\xi\sin\beta_n\eta\sin\alpha_m x_0 \times[\cos\beta_n(y_0+a_p)-\cos\beta_n y_0] \tag{11}$$

$$w_2 = \frac{2}{Db}\sum_{m=1,2}^{\infty}\sum_{n=1,2}^{\infty}\frac{\beta_n}{K'^2_{mn}}\sin\alpha_m\xi\sin\beta_n\eta(C_m) \tag{12}$$

$$w_3 = -\frac{4}{ab}\sum_{m=1,2}^{\infty}\sum_{n=1,2}^{\infty}\frac{(-1)^n\beta_n}{K'^2_{mn}}[\beta_n^2+\alpha_m^2(2-\mu)] \times\left\{\frac{1}{\alpha_m}[k_4-(-1)^m k_3]+\frac{a}{2}d_m\right\}\sin\alpha_m\xi\sin\beta_n\eta \tag{13}$$

$$w_4 = -\frac{4}{ab}\sum_{m=1,2}^{\infty}\sum_{n=1,2}^{\infty}\frac{(-1)^n\alpha_m}{K'^2_{mn}}[\alpha_m^2+\beta_n^2(2-\mu)] \times\left\{-\frac{(-1)^n}{\beta_n}k_3+\frac{b}{2}b_n\right\}\sin\alpha_m\xi\sin\beta_n\eta \tag{14}$$

$$w_5 = \frac{4}{ab}\sum_{m=1,2}^{\infty}\sum_{n=1,2}^{\infty}\frac{\alpha_m}{K'^2_{mn}}[\alpha_m^2+\beta_n^2(2-\mu)] \times[-\frac{(-1)^n}{\beta_n}k_4+\frac{b}{2}a_n]\sin\alpha_m\xi\sin\beta_n\eta \tag{15}$$

$$w_6 = 8(1-\mu)\sum_{m=1,2}^{\infty}\sum_{n=1,2}^{\infty}\frac{(-1)^n\alpha_m\beta_n}{K'^2_{mn}}[k_4-(-1)^m k_3]\sin\alpha_m\xi\sin\beta_n\eta \tag{16}$$

Eqs. (11)–(16) can be substituted into the followed boundary condition Eqs. (17)–(22).

$$\left(\frac{\partial w}{\partial\eta}\right)_{\eta=0} = 0 \tag{17}$$

$$\left[\frac{\partial^3 w}{\partial\eta^3}+(2-\mu)\frac{\partial^3 w}{\partial\xi^2\partial\eta}\right]_{\eta=b} = 0 \tag{18}$$

$$\left[\frac{\partial^3 w}{\partial\xi^3}+(2-\mu)\frac{\partial^3 w}{\partial\xi\partial\eta^2}\right]_{\xi=0} = 0 \tag{19}$$

$$\left[\frac{\partial^3 w}{\partial\xi^3}+(2-\mu)\frac{\partial^3 w}{\partial\xi\partial\eta^2}\right]_{\xi=a} = 0 \tag{20}$$

$$\left(\frac{\partial^2 w}{\partial\xi\partial y}\right)_{\substack{\xi=0\\ y=b}} = 0 \tag{21}$$

$$\left(\frac{\partial^2 w}{\partial\xi\partial\eta}\right)_{\substack{\xi=a\\ \eta=b}} = 0 \tag{22}$$

After the substitutions, Eqs. (17)–(22) will become six groups of infinite simultaneous equations which can be solved to obtain the unknown coefficients. Therefore, the deformations of each free edge can be derived.

3. Simulation and case study

According to the above theoretical analysis, the part deformations in end milling process are simulated by using FEM software ANSYS10.0 (Sun and Rong, 1990). This paper studies the small deformations for end milling of thin-walled plate, the structural static analysis is thus used to calculate the deformations. By using FE analysis, the low rigidity part is modeled as a flexible cantilever thin-walled plate. The inputs to the FE analysis include a set of parameters describing material properties, boundary conditions and other constraints. The radial cutting force is applied with the linear loads, which acts on the contact zone between the cutter and the parts. In the process of simulating, the influence of linear loads, location of the cutter (including x and y direction), thickness of the plates on the deformations of the thin-walled plates are analyzed. The flow chart applied to calculate the deformations is shown in Fig. 5.

The cutting force distributed along the cutter teeth edge is projected to the tool–part intersection line, which distribute among the nodes close to the tool–part intersection line. By using FE analysis, the deformations on every point of the thin-walled plate can be predicted. In order

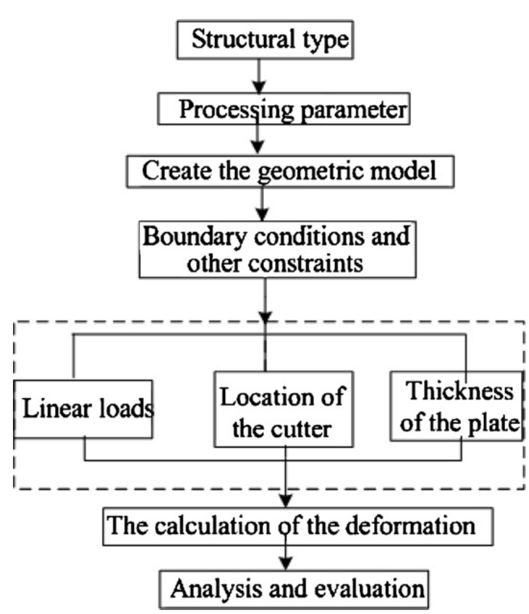

Fig. 5 – General planning of studying deformations.

to investigate the influences of the applied load, cutter location, and part thickness on the deformations of the thin-walled plate, the following three case studies are presented. The size of the thin-walled plate used in this paper is 100 mm × 100 mm × 10 mm. The material of the part is aluminum alloy with Young's modulus of 70 GPa and Poisson's ratio of 0.33. The axial depth of cut is 10 mm.

3.1. *Case one: influences of the unit linear load on the deformations of the thin-walled plates*

The cutter acts on $x = 25$ mm and $y = 75$–85 mm of the plate. The applied loads are 50, 75, 100, 150, 200, 300, and 400 N/m, respectively. In FEM analysis, the thin-walled plate is divided by the meshing. Assume that the bottom edge of the plate ($y = 0$ mm) is fixed. The thin-walled plate is exerted upon with different unit linear load. The maximal deformations can be obtained on the condition of each unit linear load. Influences of the unit linear load on the maximal deformations of the thin-walled plates are shown in Fig. 6.

Fig. 6 illustrates that the maximal deformations of thin-walled plate in end milling process are linearly increased with the higher milling force. If the unit linear load is continually increased, the deformations will go beyond the range of small deformations, which will influence the accuracy and quality of the machined part seriously. Accordingly, in end milling of thin-walled plate, appropriate cutting parameters should be selected to obtain the limited cutting force, which can ensure that the deformations of thin-walled plate are in a certain extent. Thus, it can guarantee the accuracy and quality of the machined part.

The deformations of each edge under the unit load of 100 N/m are shown in Fig. 7. Fig. 7 illustrates that the deformations have the common rules, that is to say, the part deformations are gradually increased from bottom to top. When the cutter acts on the certain location of thin-walled plate, the deformations of free angular point near to the location of cutter are the maximum. At this time, the location of the maximal deformations are at the angular point of $x = 0$ mm and $y = 100$ mm. Hence, in end milling of flexible plates, the higher the plate height is, the larger deformations the part induces. The accuracy and quality of the machined part is poorer and more difficult to control.

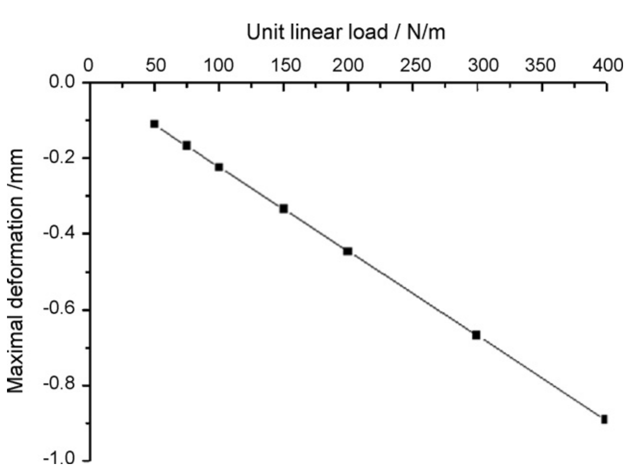

Fig. 6 – Influences of the unit linear load on the deformations of the thin-walled plates.

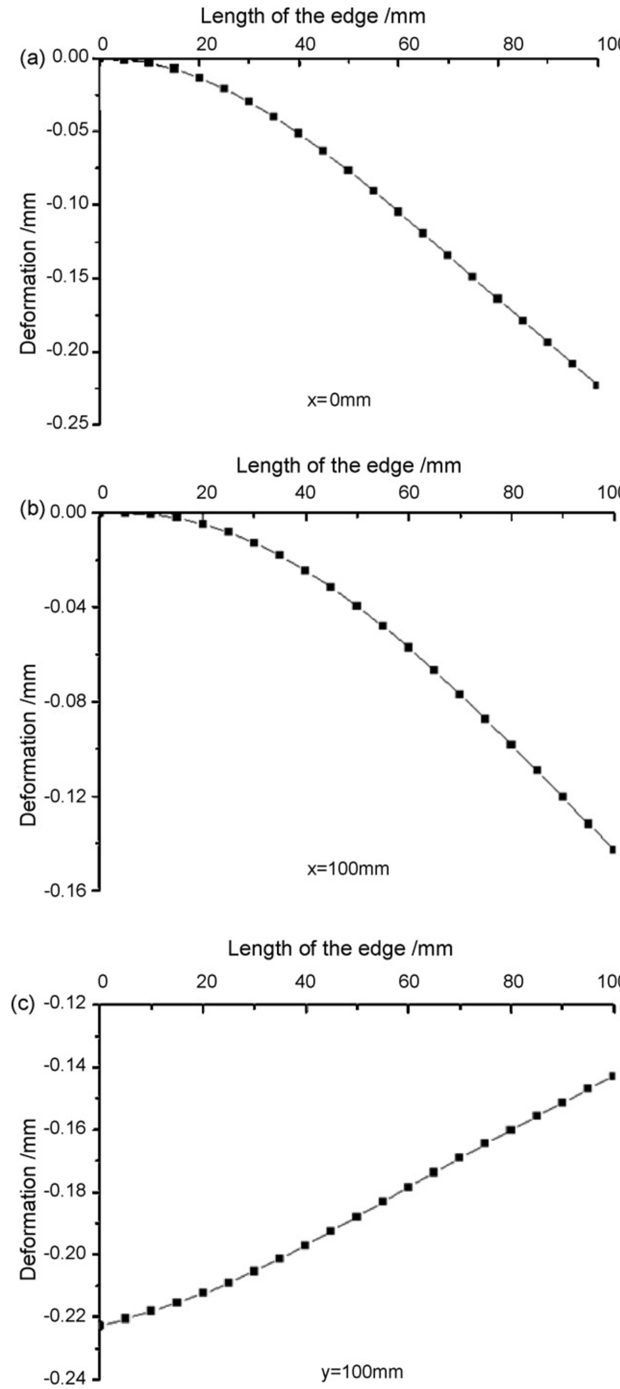

Fig. 7 – Static deformations of each edge when the unit linear load is 100 N/m.

3.2. *Case two: influences of cutter location on the deformations of thin-walled plates*

Firstly, influence of the cutter location at horizontal direction (*X*) on the deformations of thin-walled plates is presented.

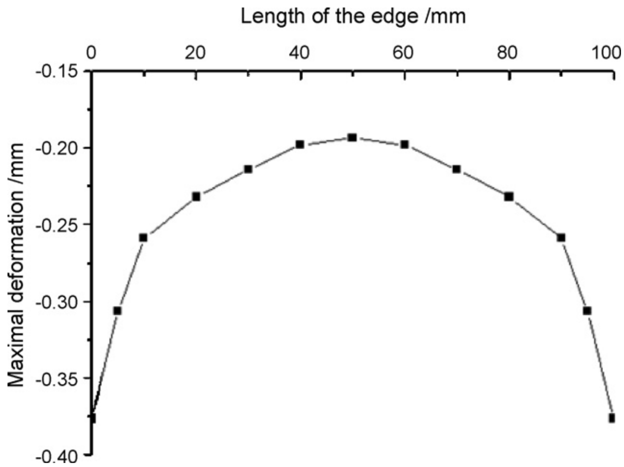

Fig. 8 – Influences of the cutter location at X direction on the deformations of the thin-walled plates.

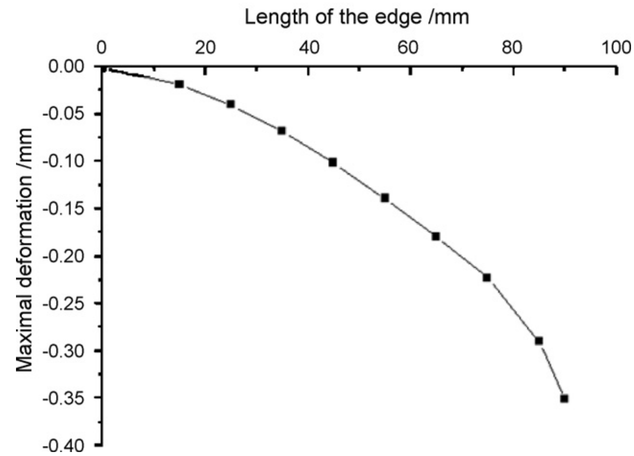

Fig. 9 – Influences of the cutter location at Y direction on the deformations of the thin-walled plates.

The unit linear load is 100 N/m. The linear load acts on $y = 75–85$ mm, while $x = 0$, 10, 20, 30, 40, 50, 60, 70, 80, 90, and 100 mm of the plate, respectively. The maximal deformations can be obtained on the condition of each cutter location. Influence of the cutter location at horizontal direction (X) on the maximal deformations of the thin-walled plates is shown in Fig. 8.

Fig. 8 illustrates that the part deformations are obvious difference when the milling cutter acts on the different location of x direction. Moreover, the deformations distribution is symmetric with respect to the middle line ($x = 50$ mm). The part deformations reach the maximum value at the location of $x = 0$ and 100 mm, while the minimum deformations are at the location of $x = 50$ mm. It is observed in Fig. 8 that the increased speed of deformations near the free edge ($x = 0$ and 100 mm) is rapider than that of the middle area.

Then, influences of the cutter location at vertical direction (Y) on the deformations of thin-walled plates are analyzed. The unit linear load is 100 N/m. The linear load acts on $x = 25$ mm, while $y = 0–10$ mm, 15–25 mm, 25–35 mm, 35–45 mm, 45–55 mm, 55–65 mm, 65–75 mm, 75–85 mm, 85–95 mm, and 90–100 mm of the plate, respectively. When the cutter moves at vertical direction (Y) of thin-walled plate, the maximal deformations can be obtained. Influence of the cutter location at vertical direction (Y) on the maximal deformations of the thin-walled plates is shown in Fig. 9.

Fig. 9 illustrates that the part deformations are gradual increased from bottom to top. When the cutter acts on the near of fixed edge ($y = 0$ mm), the part deformations are very small. While the cutter acts on the near of cantilever edge ($y = 100$ mm), the deformations reach the maximum value. Hence, in order to guarantee the accuracy and quality of the machined part, when the cutter acts on the near of cantilever edge, it should make the cutting force smaller. That is to say, the appropriate cutting parameters should be selected to guarantee the small cutting force, thus to obtain the smaller plate deformations to increase the quality of the machining part.

3.3. *Case three: influences of part thickness on the deformations of the thin-walled plates*

The unit linear load is 100 N/m and acts on $x = 25$mm and $y = 75–85$ mm of the plate. The thickness of the plate is 6, 7, 8, 9, 10, 11, 12, 13, 14, and 15 mm, respectively. According to the general planning of studying deformations, when the part thickness increase gradually from 6 to 15 mm, the maximal deformations can be obtained on the condition of every part thickness. Influence of the part thickness on the maximal deformations of the thin-walled plates is shown in Fig. 10.

As shown in Fig. 10, the maximal deformations are in inverse proportion to the wall thickness when the same unit linear load is applied. That is to say, the thinner the part thickness is, the greater the deformations are. Moreover, when the part thickness is diminished to a certain value (about 6 mm in this paper), the maximal deformations will increase rapidly. At this time, the deformations of thin-walled plate will be elastic–plastic deformations, which are not studied in this paper. Hence, in the process of milling thin-walled plate, the plate thickness is decreased gradually. If the cutting param-

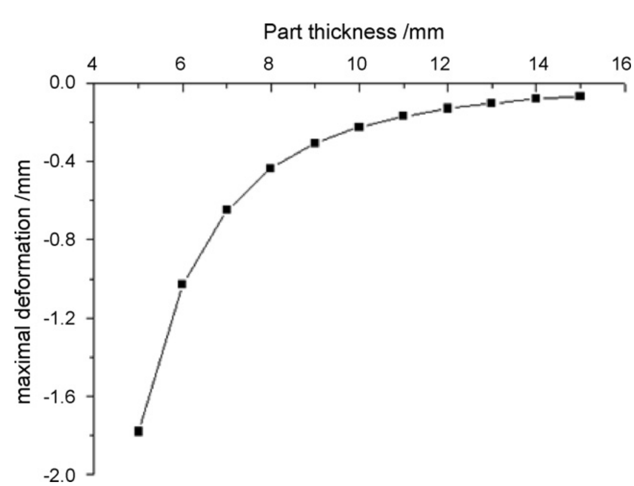

Fig. 10 – Influences of the part thickness on the deformations of the thin-walled plates.

eters hold the same value, the deformations will increase gradually with the diminished thickness.

4. Conclusions

In the process of milling thin-walled plate, the change of plate thickness is reduced gradually. Consequently, the end milling of such thin-walled plates is very complicated, which makes it even more difficult to control the accuracy of machining.

The paper has presented the deformations characteristics in end milling of thin-walled plates on the basis of reciprocal theorem. It is shown from the simulating results that the linear loads, milling cutter location and thickness of the plate have a significant impact on the part deformations. If holding the cutting parameters invariable in the process of milling the thin-walled plate, it will lead to inefficient or inaccuracy machining parts. Therefore, in the process of milling thin-walled plate, to obtain the better accuracy and quality of the machined part, the diverse cutting parameters should be selected at each layer of machining part to satisfy the demand of the smaller cutting force and machining efficiency.

REFERENCES

Budak, E., 2006. Analytical models for high performance milling. Part I. Cutting forces, structural deformations and tolerance integrity. Int. J. Mach. Tools. Manuf. 46, 1478–1488.

Erhan, B., Altintas, Y., 1995. Modeling and avoidance of static form errors in peripheral milling of plates. Int. J. Mach. Tools. Manuf. 35, 459–476.

Fu, L.B., 2003. New Theory of the Work Equality. Science Press, Beijing.

Ning, H., Zhigang, W., Chengyu, J., et al., 2003. Finite element method analysis and control stratagem for machining deformation of thin-walled components. J. Mater. Process. Technol. 139, 332–336.

Ratchev, S., Liu, S., Becker, A.A., 2005. Error compensation strategy in milling flexible thin-wall parts. J. Mater. Process. Technol. 162–163, 673–681.

Ratchev, S., Liu, S., Huang, W., et al., 2006. An advanced FEA based force induced error compensation strategy in milling. Int. J. Mach. Tools. Manuf. 46, 542–551.

Sun, J.F., Rong, W.W., 1990. Finite Element Method and its Application. Publishing Company of Beijing Aviation and Aeronautics University, Beijing.